Loop B serine of a plasma membrane aquaporin type PIP2 but not PIP1 plays a key role in pH sensing

Agustín Yaneff, Lorena Sigaut, Natalia Gómez, Cecilia Aliaga Fandiño, Karina Alleva, Lía Isabel Pietrasanta, Gabriela Amodeo

PII: S0005-2736(16)30273-5
DOI: doi: 10.1016/j.bbamem.2016.08.002
Reference: BBAMEM 82281

To appear in: *BBA - Biomembranes*

Received date: 8 April 2016
Revised date: 8 July 2016
Accepted date: 7 August 2016

Please cite this article as: Agustín Yaneff, Lorena Sigaut, Natalia Gómez, Cecilia Aliaga Fandiño, Karina Alleva, Lía Isabel Pietrasanta, Gabriela Amodeo, Loop B serine of a plasma membrane aquaporin type PIP2 but not PIP1 plays a key role in pH sensing, *BBA - Biomembranes* (2016), doi: 10.1016/j.bbamem.2016.08.002

Loop B serine of a plasma membrane aquaporin type PIP2 but not PIP1 plays a key role in pH sensing

Agustín Yaneff[a,†], Lorena Sigaut[b,c], Natalia Gómez[d], Cecilia Aliaga Fandiño[a], Karina Alleva[a,†], Lía Isabel Pietrasanta[b,c], Gabriela Amodeo[a,*]

[a]Departamento de Biodiversidad y Biología Experimental, Facultad de Ciencias Exactas y Naturales and Instituto de Biodiversidad y Biología Experimental (IBBEA), Universidad de Buenos Aires and Consejo Nacional de Investigaciones Científicas y Técnicas (CONICET), Buenos Aires, Argentina.
[b]Departamento de Física and Instituto de Física de Buenos Aires (IFIBA, UBA-CONICET), Facultad de Ciencias Exactas y Naturales, Universidad de Buenos Aires, Buenos Aires, Argentina.
[c]Centro de Microscopías Avanzadas (CMA), Facultad de Ciencias Exactas y Naturales, Universidad de Buenos Aires, Buenos Aires, Argentina
[d]Instituto de Investigaciones Farmacológicas (ININFA), Universidad de Buenos Aires and Consejo Nacional de Investigaciones Científicas y Técnicas (CONICET), Buenos Aires, Argentina.

[†]A.Y. present address is Instituto de Investigaciones Farmacológicas (ININFA, UBA-CONICET); K.A. present address is Instituto de Química y Fisicoquímica Biológica "Alejandro C. Paladini" (IQUIFIB, UBA-CONICET) and Departamento de Fisicomatemática, Facultad de Farmacia y Bioquímica, Universidad de Buenos Aires.

Corresponding author: Dr. Gabriela Amodeo, Email: amodeo@bg.fcen.uba.ar

Abstract

In the plant kingdom, the plasma membrane intrinsic aquaporins (PIPs) constitute a highly conserved group of water channels with the capacity of rapidly adjusting the water permeability (P_f) of a cell by a gating response. Most evidence regarding this mechanism was obtained by different biophysical approaches including the crystallization of a *Spinaca olaracea* PIP2 aquaporin (SoPIP2;1) in an open and close conformation. A close state seems to prevail under certain stimuli such as cytosolic pH decrease, intracellular Ca^{2+} concentration increase and dephosphorylation of specific Serines. In this work we decided to address whether the state of phosphorylation of a loop B Serine -highly conserved in all PIPs- combined with cytosolic acidification can jointly affect the gating response. To achieve this goal we generated loop B Serine mutants of two PIP types of *Fragaria x ananassa* (FaPIP2;1S121A and FaPIP1;1S131A) in order to simulate a dephosphorylated state and characterize their behavior in terms of P_f and pH sensitivity. The response was tested for different co-expressions of PIPs (homo and heterotetramers combining wild-type and mutant PIPs) in Xenopus oocytes. Our results show that loop B Serine phosphorylation status affects pH gating of FaPIP2;1 but not of FaPIP1;1 by changing its sensitivity to more alkaline pHs. Therefore, we propose that a counterpoint of different regulatory mechanisms -heterotetramerization, serine phosphorylation status and pH sensitivity- affect aquaporin gating thus ruling the P_f of a membrane that expresses PIPs when fast responses are mandatory.

Highlights

- Plant plasma membrane aquaporins, also known as PIP, are a challenging model to address how the gating mechanism affects the membrane water permeability.
- A dephosphorylated state of Loop B Serine in type PIP2 aquaporins contributes to shifting the closure of the channel towards more alkaline pH.
- Membranes that express PIP aquaporins can combine heteromerization, phosphorylation status and pH sensitivity to rapidly adjust membrane water permeability when fast responses are mandatory.

1. Introduction

Certain cellular processes in organisms of all kingdoms demand adjustments in the plasma membrane permeability to water and/or small-uncharged solutes [1–3]. A change in membrane permeability not only affects the exchange capacity (in terms of quantity, *i.e*. solute/water concentration changes) but also the rate of this exchange (how fast is the conduction, *i.e*. time scale of the process). During the last 25 years aquaporins have become important protagonists of many of these processes, particularly for those that request a high exchange rate of water and/or small-uncharged solutes [3,4].

Structural studies on aquaporins from a vast range of organisms revealed that these proteins share a conserved tetrameric structure [5]. Each of the monomers of this tetramer forms a narrow water-conducting channel surrounded by six transmembrane helices. The pore region is delimited by a seventh pseudo-transmembrane segment formed by the dipping of cytoplasmic loop B and extracellular loop E into the membrane creating two shorter helices. Along the water-conducting channel, two regions are part of the channel signature: the NPA-region in the center of the channel

and the aromatic-arginine (ar/R) motif closer to the extra-vestibular region, known as the selectivity filter.

Among the described regulatory mechanisms, channel gating provides the fastest response to change water membrane permeability (P_f) since other mechanisms -such as trafficking or transcriptional regulation- are comparatively slower. In particular, PIPs constitute a highly conserved group of plant aquaporins whose gating ability has been extensively studied. X-ray crystal structures of SoPIP2;1 obtained in different conditions and molecular dynamics simulations lead to the proposal of a gating mechanism in which loop D inserts into the cavity of the channel occluding the water pore [6]. This rapid adjustment of the water membrane permeability in PIPs was studied under specific stimuli: i) cytosolic acidification [7–10]; ii) specific dephosphorylation of Serine residues [6,11–13]; iii) modulation of intracellular calcium concentration [14,15]. Supplementary Fig. 1B, C, D shows an homology model of FaPIP2;1 where the main residues involving this mechanism are shown.

The effect of cytosolic acidification on gating of PIPs has been studied both in native membranes [7,14,16,17] and in different aquaporins overexpressed in heterologous systems [7,8,15,18,19]. The discovery of a highly conserved Histidine residue (His193 in AtPIP2;1 of *Arabidopsis thaliana*) responsible for the PIP gating was a clear landmark in the field [7]. As mentioned before, both structural studies as well as molecular dynamics simulations have contributed to propose the conformational changes that lead to the gating process: at low pH the His193 is protonated and promotes the channel capping by loop D [6,9].

Serine phosphorylation is a common post-translational modification involved in gating and trafficking in membrane channels in general [20,21]. The first report of PIP Serine phosphorylation has established that two Serines, Ser115 located in loop B and Ser274 in the C-terminal of SoPIP2;1, are responsible for channel activity when expressed in *Xenopus laevis* oocytes [11]. In the case of the loop B Serine, the influence of its phosphorylated state on channel activity was mainly investigated in the

PIP subgroup known as PIP2. When expressed in various heterologous systems, the mutation of this Serine to Alanine produced a partial [12,22,23] or a total reduction [18,24,25] of the membrane water permeability compared to the wild-type. However, in most cases the amount of protein located in the plasma membrane was not tested and thus, the observed total or partial blockage could be attributed to an alteration of PIP trafficking to plasma membrane.

On the other hand, the Serine located in the C-terminal domain was studied by mutations performed in Ser274 of SoPIP2;1 or Ser285 of *Zea mays* (ZmPIP2;1) to Alanine and in both cases water transport is reduced. The authors suggested that these particular Serines might also contribute to the channel opening mechanism [11,23]. However, this C-terminal Serine is not present in several PIP2 and PIP1 aquaporins and therefore it is not as conserved as the above-mentioned loop B Serine (Supplementary Fig. 1A).

Until now, it has not been addressed if these two conserved features (phosphorylation and pH sensitivity) might act cooperatively in the gating response. Thus, the goal of this work is to disclose the role of loop B Serine on gating and to address, if (and how) its state of phosphorylation affects gating triggered by cytosolic acidification. The strength of the PIP gating modified by cytosolic acidification depends on the wide range of combinatory features that contribute to close the channel [10,26]. Previous works have demonstrated that PIPs also shift pH sensing to more physiological values by means of heteromerization of specific subgroups: PIP1 and PIP2 [8,10,26].

Under this scenario, our proposal is to analyze the influence of the state of phosphorylation of loop B Serine on PIP pH sensing. Our hypothesis is that dephosphorylated serine favors channel closure at acidic pH and shifts the EC_{50} toward more alkaline values. If the channel closure is at a more acidic pH it is less feasible to occur in physiological conditions due to the high buffering capacity of intracellular pH that will prevent the cytosol from achieving these values. In physiological conditions, the cytosolic pH is considered to remain slightly alkaline between 7.2-7.5 values, while

both the vacuole and external (apoplastic) pH are always acidic (pH 5.0-6.0) [27]. The cytosol has a much tighter buffer capacity (20 to 80 mM of H^+ per pH unit), but these range values are sufficiently enough to be sensed by PIP aquaporins. Thus, any condition that contributes to shift the EC_{50} of the response to more alkaline pH values favors a rapid change in the rate of water exchange that will be reflected in the membrane water permeability. We think that our working hypothesis together with evidence obtained through phosphoproteomics analysis -confirming that this Serine is found in a dephosphorylated state- [11,23,28–33] might bring light to the relevance of the PIP pH gating mechanism in adjusting plasma membrane water permeability in plant cell processes.

2. Materials and Methods

2.1 Genetic constructions

Plasmid constructions pT7Ts-*Fa*PIP2;1, pT7Ts-*Fa*PIP2;1-EYFP and pT7Ts-*Fa*PIP1;1 generated in previous work [10,34,35] were used. Mutated pT7Ts plasmids encoding FaPIP2;1S121A, FaPIP1;1S131A and FaPIP2;1S121A-EYFP were obtained by site direct mutagenesis (QuickChange, Stratagene, USA) using custom-made oligonucleotide primers (Eurofins MWG Operon, USA). All the constructs were confirmed by DNA sequencing (Macrogen Inc. Maryland, USA).

2.2 In vitro synthesis and translation

Capped complementary cRNA encoding FaPIP1;1, FaPIP2;1, FaPIP2;1S121A, FaPIP1;1S131A,FaPIP1;1-EYFP, FaPIP2;1-EYFP and FaPIP2;1S121A-EYFP were synthesized in vitro using the mMESSAGE mMACHINE T7 High Yield Capped RNA Transcription Kit (Ambion, Austin, TX, USA). The pT7Ts derived vectors carrying the corresponding sequence as templates were linearized employing XbaI. The synthesized products were suspended at a final concentration of 0,1 μg μL^{-1} in RNAse-

free water supplemented with Recombinant RNAsin (Ribonuclease inhibitor, Promega, USA) and stored at -20 ºC until used. The cRNA was quantified by fluorescence using Quant-iT RNA Assay Kit (Invitrogen, UK). The quality of cRNA was checked by agarose gel electrophoresis and GelRed staining (BioAmerica Biotech Inc., USA). At least two independent cRNA syntheses were assayed.

2.3 Oocyte transport studies

Defolliculated Xenopus oocytes were injected using an automatic injector (Drummond Scientific Co., Broomall, PA) and then incubated for 72 hours at 18°C in ND96 medium (96 mM NaCl, 2 mM KCl, 1 mM $MgCl_2$, 1.8 mM $CaCl_2$ and 5 mM HEPES pH 7.5; ~200 mOsmol kg^{-1} H_2O) supplemented with 1 µg ml^{-1} gentamycin sulfate.

Osmotic water permeability coefficient (P_f) was determined by measuring the rate of oocyte swelling induced by a hypo-osmotic shock of 160 mOsm kg^{-1}. Changes in cell volume were video monitored by a Life CamVX-3000 color videocamera (Microsoft, CA, USA) attached to a zoom stereo-microscope (Olympus SZ61, Olympus Co., Tokyo, Japan). The cell swelling was video-captured in still images (each 10 s during 60 s) using the AMCaP version 9.20 and then the images were analyzed by treating each oocyte image as a growing sphere whose volume could be inferred from its cross-sectional area (software Image J version 1.37, http://rsb.info.nih.gov/ij). The osmotic water permeability (P_f) was calculated according previous reports [36,37]. All osmolarities were determined using a vapor pressure osmometer (Vapro 5520C Wescor, Logan, UT). Non-injected oocytes were used as a negative control [35]. Results from experiments performed with different oocytes batches were not pooled; therefore, all of the experiments shown are representative for at least three different experiments.

2.4 Confocal Microscopy

Confocal fluorescence microscopy was used to determine the localization of the respective aquaporins tagged with EYFP in *Xenopus laevis* oocytes. As a marker of the interior of the oocyte we used tetrametylrhodamine (TMR) dextran (10,000 MW;

Invitrogen-Molecular Probes, USA) [10]. Three days after cRNA injection and 40 min prior to imaging, oocytes were microinjected with 50 nl of a 33 μM aqueous solution of TMR-dextran. Fluorescence images of EYFP distribution, together with TMR, were obtained with a FluoView1000 spectral confocal scanning microscope (Spectral FV1000 Olympus, Japan), using a 60X UPLSAPO oil immersion objective lens with a numerical aperture of 1.35. To avoid crosstalk, images were recorded line by line in a sequential order. EYFP and TMR were excited using the 488 nm line of the argon laser and the 543 nm He-Ne respectively, and the emitted fluorescence was detected in the 500–530 nm and 570–670 nm range. Autofluorescence (monitored in control non-injected oocytes) was negligible compared to cells expressing fluorescent PIP.

Intensity profiles were generated with the program ImageJ (http://rsb.info.nih.gov/ij/) and then analyzed with Origin (OriginLab, Northampton, MA). These profiles were obtained averaging consecutive pixels over 5 μm for both signals (EYFP-aquaporin and TMR-dextran) along the direction perpendicular to the PM. The normalized intensity profile for each channel was calculated by subtracting the baseline and dividing by the maximum intensity of the profile. The difference profile was calculated as the difference between the normalized EYFP-aquaporin and TMR-dextran profiles. For each image, three different regions were analyzed, and the average difference profile was employed to infer the aquaporin localization. Subcellular aquaporin localization was studied in oocytes expressing FaPIP1;1, FaPIP2;1 or FaPIP2;1S121A, or co-expressing two of them as indicated in the Figures. For each condition we analyzed 3–6 oocytes of at least 2 donor frogs, and an average difference profile was calculated. The average difference profiles for each studied condition are shown as supplementary information.

2.5 Aquaporin inhibition by pH and by K252a

The oocyte cytosolic pH was modified following the protocol described in Tournaire-Roux (et al. 2003) [7]. Briefly, oocytes were pre-incubated in different Sodium Acetate (NaAc) solutions with distinct final pH. For the 5.8-6.8 pH intervals, the NaAc solutions

were: 50 mM NaAc, 20 mM MES, supplemented with mannitol 1 M to adjust osmolality to ~200 mOsmol kg^{-1} H_2O and supplemented with Sodium Hydroxide (NaOH) to adjust final pH. For the 6.8-7.6 pH range, the NaAc solutions were: 50 mM NaAc, 20 mM HEPES, supplemented with mannitol 1 M to adjust osmolality to ~200 mOsmol kg^{-1} H_2O and supplemented with NaOH to adjust final pH. The pH of each solution was controlled prior the swelling assay. The swelling response was performed by transferring the oocyte to the same NaAc incubation solution diluted five-fold with distilled water in order to induce the osmotic shock. To calculate internal proton concentration ($[H^+]_{int}$) we used a calibration curve described before [8]. The results of P_f values for each $[H^+]_{int}$ were fit with the following sigmoidal dose-response equation using GraphPad Prism 6 [10]:

$$P_f = \frac{(P_f MAX - P_f min) \times [H^+]_{int}{}^h}{(K_I{}^h + [H^+]_{int}{}^h)} + P_f min \quad \text{Equation 1}$$

Where P_fMax is the fitting parameter representing the highest P_f achieved, $P_f$min is the fitting parameter representing the lowest P_f achieved, K_I is the $[H^+]$ at which half of the maximum effect occurs and *h* is the Hill coefficient. Results from experiments performed with different oocyte batches were not pooled; therefore all the dose-response curves shown in this work are representative for at least three different curves. For each condition, a K_I mean value (K_I ± SEM, n = 3-5) and an EC_{50} mean value calculated from the independent K_I values (EC_{50} ± SEM, n = 3-5) are shown.

To test the effect of K252a and/or pH inhibition, oocytes were incubated for 30 min in iso-osmotic NaAc solutions with different pH containing 1 μM K252a (Sigma-Aldrich) and DMSO 0.1%. Control experiments were performed incubating the same time period with a NaAc Solution with DMS0 0.1%.

2.6 Statistical analysis

The results are reported in the form of means ± SEM. Significant differences between treatments were calculated using Student's t-test using GraphPad Prism 6.

3. Results

3.1 Synergic effect of K252a and a decrease in cytosolic pH in FaPIP2;1 water transport

Our first approach was to explore how the phosphorylated state of loop B Ser121 (equivalent to SoPIP2;1 Ser115, Supplementary Fig. 1) affects pH gating of PIP aquaporins by incubating the oocytes overexpressing FaPIP2;1 in the presence of K252a, a compound that inhibits certain protein kinases. The results showed that oocytes incubated at pH_i=7.4 and treated with 1 μM K252a do not produce any significant change in the P_f (147 ± 12 10^{-4} cm s^{-1}) compared to control P_f values (193 ± 23 10^{-4} cm s^{-1}) (Fig. 1A). While a similar result was previously observed for *Camelina sativa* CsPIP2;1 [12], other reports showed that K252a caused a decrease in the P_f of oocytes expressing another PIP2 [11,22,23]. We also tested the pH inhibitory effect at pH_i=6.6 (by incubating oocytes at pH=6.3 in a sodium acetate solution). At this pH value the P_f of oocytes expressing FaPIP2;1 was not inhibited ([10], Fig. 1A, B, 5A). Interestingly, when oocytes expressing FaPIP2;1 were incubated at this pH in combination with 1 μM K252a, a significant decrease in the P_f was observed ($p<0.05$, n=8-12). Upon this inhibition, we decided to test whether there was a cooperative response between K252a and gating due to Histidine protonation. Fig.1B shows P_f vs. $[H^+]_i$ dose–response curves for oocytes injected with FaPIP2;1 cRNA subjected or not to 30 minutes incubation with 1 μM K252a. Upon treatment with K252a 1 μM, K_I was shifted to lower [H+] significantly ($p<0.005$, n=3-5) compared with controls (Fig. 1D).

3.2 Characterization of activity and trafficking of FaPIP2;1S121A mutant

We generated a FaPIP2;1 mutant replacing Serine 121 with Alanine (FaPIP2;1S121A). We characterized FaPIP2;1S121A biological activity by means of swelling assays and protein localization within the oocyte. Fig. 2A shows P_f measurements on Xenopus oocytes injected with different masses of cRNA coding for FaPIP2;1S121A. The P_f of oocytes expressing FaPIP2;1S121A is significantly different from non-injected oocytes

only considering oocytes injected with very high amounts (10 ng) of cRNA ($p<0.05$, n=11-13). We generated a fluorescent tagged PIP (FaPIP2;1S121A-EYFP) in order to test if this mutant localizes or not at the plasma membrane. To infer subcellular localization, intensity profiles were analyzed and compared to average difference profiles for oocytes expressing FaPIP1;1-YFP or FaPIP2;1-EYFP (Fig. 2D), which were used as a reference for interior localization or plasma membrane localization, respectively (Supplementary Fig. 2).

When low amounts of cRNA of the EYFP labeled mutant are injected into the oocyte, the EYFP fluorescence is more compatible with signal restricted to internal structures (Fig. 2B and 2E). However, if the amount of injected cRNA is increased, fluorescent signal is more probable to be detected at the plasma membrane (Fig. 2C and 2F). Summarizing these results, the low water transport detected in oocytes expressing FaPIP2;1S121A (Fig. 2A) could be attributed to an impairment of FaPIP2;1S121A to correctly achieve the plasma membrane.

To surpass this inconvenience we employed a strategy reported in other works [10,38] and tested whether the co-expression of FaPIP2;1S121A with FaPIP2;1 wild-type can overcome the difficulty of the mutant to reach the plasma membrane. Fig. 3A shows that oocytes co-expressing FaPIP2;1S121A with FaPIP2;1 in equal amounts of RNA (1.25 ng + 1.25 ng) presented a P_f greater than the obtained by the injection of 1.25 ng of RNA of FaPIP2;1 alone ($p<0.005$, n=10-15) but not significantly different to the P_f that resulted from the injection of 2.5 ng of FaPIP2;1 (n=10-15). Moreover, FaPIP2;1S121A-EYFP is always localized in the plasma membrane when co-expressed with FaPIP2;1 (a representative case is shown in Fig.3B). This result confirms that the difficulties of FaPIP2;1S121A in achieving the plasma membrane were overcome when it is interacting with FaPIP2;1 wild type.

Since it was previously described that FaPIP2;1 and FaPIP1;1 can form heterotetramers [10], we decided to tested the interaction between FaPIP2;1S121A and FaPIP1;1. Fig.4A shows that the P_f of oocytes that co-expressed FaPIP1;1 with

FaPIP2;1S121A in a 3:1 ratio is significantly different from the P_f exhibited by oocytes expressing FaPIP2;1S121A alone ($p<0.005$, n=8-12), proving that both channels interact as reported for FaPIP1;1 and FaPIP2;1 wild type [10,35]. Moreover, the interaction of both proteins can be confirmed tracking their localization in the oocyte. When expressed alone, FaPIP2;1S121A-EYFP is less probable to be found at the plasma membrane and FaPIP1;1-EYFP [10] is unable to reach the plasma membrane. However, when FaPIP2;1S121A-EYFP was co-expressed with FaPIP1;1 or FaPIP2;1S121A with FaPIP1;1-EYFP, the fluorescent signal corresponding to the tagged FaPIP2;1 and FaPIP1;1 respectively, is always localized at the plasma membrane (Fig. 4A, 4B, Supplementary Figure 2).

3.3 Channel gating triggered by changes in the cytosolic pH is more sensitive for FaPIP2;1S121A than for FaPIP2;1.

Once FaPIP2;1S121A was characterized, we proceeded to assess whether the mutation affects gating triggered by cytosolic acidification. Fig.5A shows P_f vs. $[H^+]$ dose-response curves for FaPIP2;1 and FaPIP2;1S121A. Interestingly, the inhibition curve produced by cytosolic acidification of FaPIP2;1S121A is shifted to lower proton concentration values compared to FaPIP2;1 curve. This effect is also reflected in the showed mean EC_{50} values for each K_I (Fig. 5B). While FaPIP2;1 EC_{50} is 6.51 ± 0.01, the FaPIP2;1S121A EC_{50} resulted to be significantly different (6.70 ± 0.02; n=3-5, $p<0.005$).

3.4 Disclosing the role of loop B serine in gating of FaPIP2;1 and FaPIP1;1 when co-expressed

As mentioned before, heteromerization plays a key role in pH gating, and it was shown that the interaction of FaPIP1;1 with FaPIP2;1 produces a shift in the pH inhibition towards more physiological values when compared with FaPIP2;1 alone. Since our results show that the loop B Serine mutation affects also PIP gating, we investigated the effect on the EC_{50} value when co-expressing FaPIP2;1S121A with FaPIP1;1. Fig.

6A shows that the inhibition curve obtained for the FaPIP1;1:FaPIP2;1S121A co-expression in a 3:1 ratio is shifted to even more alkaline values in comparison with the curve obtained for FaPIP1;1:FaPIP2;1 in a 3:1 ratio. The EC_{50} values presented in Fig. 6B are 6.60 ± 0.02 for FaPIP1;1-FaPIP2;1 co-expression and 6.78 ± 0.03 for FaPIP1;1-FaPIP2;1S121A co-expression. Means are significantly different (n=4, $p<0.005$).

Finally, we considered important to test if the equivalent mutation in FaPIP1;1 would have the same effect in modifying the sensitivity to pH gating. For that purpose we generate a PIP1 mutant (FaPIP1;1S131A) and studied its interaction with FaPIP2;1. Fig. 7A shows that FaPIP1;1S131A:FaPIP2;1 co-expressed in a 3:1 ratio modified the oocyte P_f significantly compared to the exhibited by FaPIP2;1 injected alone ($p<0.05$, n= 8-12). These observations are in agreement with a PIP1-PIP2 interaction. Then, we analyzed if the mutation affects the gating response to a decrease of cytosolic pH. Fig. 7B shows that the P_f vs. $[H^+]$ dose–response curves of FaPIP1;1:FaPIP2;1 co-expression and FaPIP1;1S131A:FaPIP2;1 co-expression (both in a 3:1 ratio) are similar. In fact, the EC_{50} value for FaPIP1;1S131A-FaPIP2;1 co-expression is 6.59 ± 0.01 and is not significantly different from the FaPIP1;1-FaPIP2;1 EC_{50} value already given. Apparently, the state of phosphorylation of this PIP1 loop B Serine does not affect the sensitivity to a decrease in cytosolic pH, in contrast to what it is observed with FaPIP2;1.

4. Discussion

In this work, we addressed the possibility that the state of phosphorylation of a loop B Serine conserved in all PIPs affects the gating response caused by changes in cytosolic pH. For this purpose we used two types of aquaporins (FaPIP2;1 and FaPIP1;1) which have been extensively characterized in terms of their intrinsic properties and response to pH [10,34,35]. Our approach was to mutate this residue in both aquaporins changing Serine for Alanine in order to simulate the dephosphorylated status, and thus ensure that all the species were in the same state. Thus, we

generated FaPIP2;1S121A and FaPIP1;1S131A. Equivalent mutations had already been studied in other PIP2 and PIP1 of other plant species with dissimilar results. In some cases, it has been reported that the mutants failed to increase the oocyte P_f compared to the controls [18,24,39] while in others, P_f was lower compared to the corresponding wild-type but still significantly higher than controls [22,23,40]. This mutation was also recently performed in ZmPIP2;5 in order to prevent transport of H_2O_2, stating that it generates a non-functional channel [25]. As mentioned before, the dissimilar results could reflect trafficking failure to the oocyte membrane or a decrease of tetramers intrinsic permeability. Here we proved that the S121A mutation in FaPIP2;1 produces a functional water channel that has a deficiency in its trafficking to the plasma membrane in Xenopus oocyte system (Fig. 2 and Suppl. Fig. 2). Plasma membrane localization in Xenopus oocytes is essential to characterize the water transport capacity of the aquaporin that is being studied, but it does not necessarily reflect the protein trafficking at the plant cell level. Our results show that when FaPIP2;1S121A cRNA is injected in low amounts, there is no significant increase in the oocyte P_f compared to control (non-injected oocytes) and we also confirm that the protein produced is mostly located in Xenopus oocyte internal structures. However, if the injected amount of FaPIP2;1S121A cRNA is increased, a plasma membrane localization is more likely to be appreciated and this is consistent with an increment in the oocyte P_f (Fig. 2). Contextualizing this result, it is feasible that previous loop B serine mutations failed to increase P_f due to a lack of enough protein at the level of the plasma membrane [18,24]. This impairment to achieve the plasma membrane could be attributed to changes in the affinity of the homotetramer for any of the proteins that compose the plasma membrane trafficking system -promoted by Serine for Alanine mutation- which is amended by increasing the amount of aquaporin expressed (Fig. 2) or by the co-expression with FaPIP2;1 or FaPIP1;1 wild-type as shown in Figs. 3 and 4. In mammals, AQP2 is a clear example of how the phosphorylation of Serine residues located in kinase consensus sites can determine the subcellular localization of

aquaporins. AQP2 PKA dependent phosphorylation of Serine 256 plays a critical role in transporting to the apical membrane of epithelial cells of the kidney collecting duct [20]. Indeed, there is evidence that only one monomer of the aquaporin tetramer must be phosphorylated for proper targeting to plasma membrane of Xenopus oocytes [41]. In our case, the mutant FaPIP2;1S121A is properly targeted to plasma membrane when is forming heterotetramers with FaPIP2;1 or FaPIP1;1 wild-type (Fig. 3, 4). Stoichiometry of phosphorylated and non-phosphorylated monomers within the tetramer may be playing a key role in this process. Other features of the quaternary structure of the tetramer may be critical, since FaPIP1;1 and FaPIP2;1S121A do not reach plasma membrane efficiently when expressed separately but their heterotetramers do target to the plasma membrane (Fig. 4). Our strategy of co-expressing the mutant to guarantee its localization is in agreement with previous evidence. For example, ZmPIP2;5S121A was able to deliver ZmPIP1;2 to the plasma membrane of yeast cells used as expression system [25].

Comparing results, P_f of oocytes co-injected with FaPIP2;1S121A and FaPIP2;1 cRNA was not significantly different to the P_f of oocytes injected only with FaPIP2;1 cRNA, keeping constant the total amount of RNA injected. However, oocytes co-expressing either FaPIP2;1S121A:FaPIP1;1 or FaPIP2;1:FaPIP1;1S131A presented less water transport capacity than the FaPIP2;1:FaPIP1;1 co-expression. This could indicate that the state of phosphorylation of this residue in both FaPIP1;1 and FaPIP2;1 could be important in the P_f enhancement [10] when aquaporins form heterotetramers. In agreement with this result, previous work done with *Mimosa pudica* aquaporins have shown that the S131A mutation in MpPIP1;1 affects P_f enhancement produced by its interaction with MpPIP2;1 [39].

As explained in the introduction, at least three biochemical signals are capable of producing PIP gating (pH, calcium levels and the phosphorylation status of conserved residues). All of them seem to produce the same outcome: loop D is subject to conformational changes and occludes the water pore at the cytosolic side. In this

context, it is expected that the biochemical signals might also interact: the activation or inactivation of one of them increases or decreases the probability of the gating produced by the other. This is a common phenomenon occurring in several channels. For example, in BK K^+ channels, Ca^{2+} binding shifts voltage dependence of channel opening toward less positive voltages, while depolarization enhances the apparent affinity and cooperativity of Ca^{2+} binding [42].

Some interaction of Ca^{2+} and pH dependent gating were previously studied in PIP2 aquaporins. His199 of AtPIP2;1 which was already established as the pH sensor [7] participates also in Ca^{2+} inhibition, because its mutation alters both processes [15]. Also, the mutation of two amino acids of the divalent binding site -Asp28 and Glu31- altered pH sensitivity.

The crystallization of SoPIP2;1 in different conditions and some *in silico* experiments have contributed to deeply explore PIP2 gating in terms of phosphorylation of Serines and pH sensitivity [6,9]. It is important to complement this information with functional *in vitro* experiments. Our strategy was therefore to combine two complementary approaches: i) kinase inhibition by K252a, which favors the dephosphorylated state of Serines and ii) cytosolic acidification, that triggers a diminution of the P_f of oocytes expressing FaPIP2;1. The K252a is a pharmaceutical compound that inhibits several kinases including PKA and PKC, and it was proven for some PIP2 that its effect is specific for loop B serine phosphorylation [11,22,23]. We also characterized pH inhibition of oocytes expressing FaPIP2;1S121A by measuring its EC_{50}. Both pharmacological and mutational approach resulted in a shift of EC_{50} towards more alkaline values (Figs. 1, 5), indicating that loop B Serine dephosphorylation favors the close state at more alkaline pH. Regarding this, the EC_{50} shift observed when using the pharmacological inhibitor (Fig. 1) is of lesser magnitude than the reported for the oocytes expressing the mutant FaPIP2;1S121A (Fig. 5). Pharmacological inhibition (if compared with experiments performed with mutants) has the advantage that the amino acid residue remains unaltered, but has the disadvantage that its effect is not

complete, meaning that there will be some PIP2 with loop B Serine phosphorylated (a condition that is completely discarded if there is a mutation). It is also possible that kinase inhibition prompted by K252a is affecting the phosphorylation of other residues that generate aquaporins with a different EC_{50} shift.

Crystallization SoPIP2;1 at pH=6 allowed more insight into possible interactions of the protonated Histidine of loop D that would favor keeping the channel in the closed conformation [9]. Without Cd^{2+} in the binding site, the side chain of His193 of SoPIP2;1 is thought to interact by hydrogen bonds through a water molecule with the amide nitrogen of Ser115 and the carbonyl oxygen of Lys113. On the other hand, in the presence of Cd^{2+} on the binding site, His193 side-chain might be interacting with Asp28. When molecular dynamics simulation was done phosphorylating Ser115 residue of SoPIP2;1, a displacement of Cd^{2+} towards the periphery was seen [6]. Also, phosphate group of Ser115 started to coordinate with Cd^{2+}. Based on evidence collected for FaPIP2;1, we think that both configurations (regarding interactions of His199 of FaPIP2;1) are likely to occur with Ser121 in the phosphorylated state, but they might occur with less affinity due to the spatial modifications caused by the phosphate group. In another words, un-phosphorylated state would favor these interactions to occur, shifting the sensibility to lower $[H^+]$ concentrations.

Last but not least, this work contributes to disclose the role of loop B serine mutation between FaPIP1 and FaPIP2. We observe different behaviors when analyzing the response to cytosolic acidification of the co-expressions FaPIP2;1S121A:FaPIP1;1 and FaPIP2;1:FaPIP1;1S131A (Figs. 6, 7) compared to the co-expression FaPIP1;1:FaPIP2;1. In the first case, heterotetramerization with FaPIP2;1S121A produced an even higher shift of the EC_{50} towards alkaline values than the one produced if we compared FaPIP2;1 with FaPIP2;1S121A. In the second case no effect was observed.

The presence of a mutant FaPIP2;1S121A in the conformation of a heterotetramer modifies the gating response by shifting the dose-response curve towards more

alkaline pH. On the contrary, there are no significant differences between the EC_{50} of the co-expressions FaPIP2;1:FaPIP1;1S131A and FaPIP2;1:FaPIP1;1. This suggests that the lack of phosphorylation of FaPIP1;1 does not affect the gating sensitivity of FaPIP1;1, and does not modify FaPIP2;1 gating while interacting. It can be speculated that unlike the case of a PIP2 type aquaporin, FaPIP1;1 is not phosphorylated in the oocyte at residue 131, and thus, the mutation of this residue by Alanine did not change the behavior compared to the wild-type. In another overexpression system -COS7 cells-, it was demonstrated that MpPIP1;1 (a PIP1 from *Mimosa pudica*) was phosphorylated in this residue while MpPIP2;1 was not [39]. It is also possible that unlike what happens with FaPIP2;1, the phosphorylation of Ser131 of FaPIP1;1 produces no changes in the sensitivity to gating by cytosolic acidification.

5. Conclusion

We propose that Loop B serine of the PIP2 aquaporin is relevant in terms of pH sensing. As heteromerization is very likely to occur in plant cells, the conformation of the tetramer would make a difference not only because of the monomers involved but also because of the state of Loop B Serines that might cooperatively interact in the gating response. The physiological role of PIP closure under cytosolic acidification was subject to discussion as the study of PIPs was performed employing an heterologous system, and it was necessary to reduce cytosolic pH to values that may not be feasible in native cells [7,8,10,26,38]. When the P_f was measured on isolated vesicles of a purified fraction of plasma membrane of both red beet and Arabidopsis, the pH of half inhibition (EC_{50}) was higher and closer to physiological pH values of a plant cell [14,16]. These values are much in agreement with the changes in EC_{50} we observed in our work. There are reports that in certain conditions, both biotic and abiotic stress may cause a cytosolic acidification [43,44] and new emerging techniques have proven that there are pH microdomains within plant cells [45,46]. It is therefore possible to expect

intracellular zones with a lower pH and that this will increase the probability to find a higher population of PIPs in a closed conformation.

Many environmental stimuli as well as nutritional changes induce changes by either increasing or decreasing the phosphorylation of C-terminal residues [28,30–32,47–49]. Phospho-proteomic analysis on *Arabidopsis thaliana* and *Oryza sativa* provide strong evidence that C-terminal Serines are found in a phosphorylated state [29,50–52]. On the other hand, only few reports detected serine phosphorylation in loop B [13,53,54] and thus a dephosphorylated state seems to prevail in this Serine. The phosphorylation of the loop B Serine was detected in the presence of specific stimuli and in a certain organ [13,53]. These observations favors the hypothesis that PIP2 phosphorylation in this residue is only triggered by a precise stimulus probably linked to water homeostasis at the cellular level. If PIP2 appears mostly dephosphorylated in this residue *in planta*, pH regulation resurfaces as a regulatory mechanism with physiological relevance. The change in sensitivity to pH produced by phosphorylation of this residue provides a new level of regulation in the transport capacity of water and solutes of plant plasma membranes.

Acknowledgements

We thank to Andrea Beltrán González, Daniel Calvo and Andrea Dengis for their help.

This work was supported by the the Agencia Nacional para la Promoción Científica y Técnica [Préstamo BID PICT14-0744]; Consejo de Investigaciones Científicas y Técnicas (CONICET) Proyecto de Investigación Plurianual (PIP12-14) and Universidad de Buenos Aires UBACyT14-17, all grants to G.A. and UBACyT 20020120100155BA, grant to L.I.P.

References

[1] A. Madeira, T.F. Moura, G. Soveral, Detecting aquaporin function and regulation, Front. Chem. 4 (2016). doi:10.3389/fchem.2016.00003.

[2] P. Kitchen, R.E. Day, M.M. Salman, M.T. Conner, R.M. Bill, A.C. Conner, Beyond water homeostasis: Diverse functional roles of mammalian aquaporins, Biochim. Biophys. Acta - Gen. Subj. 1850 (2015) 2410–2421. doi:10.1016/j.bbagen.2015.08.023.

[3] C. Maurel, Y. Boursiac, D.-T. Luu, V. Santoni, Z. Shahzad, L. Verdoucq, Aquaporins in Plants., Physiol. Rev. 95 (2015) 1321–58. doi:10.1152/physrev.00008.2015.

[4] K. Alleva, O. Chara, G. Amodeo, Aquaporins: Another piece in the osmotic puzzle, FEBS Lett. 586 (2012) 2991–2999. doi:10.1016/j.febslet.2012.06.013.

[5] S. Kreida, S. Törnroth-Horsefield, Structural insights into aquaporin selectivity and regulation, Curr. Opin. Struct. Biol. 33 (2015) 126–134. doi:10.1016/j.sbi.2015.08.004.

[6] S. Tornroth-Horsefield, Y. Wang, K. Hedfalk, U. Johanson, M. Karlsson, E. Tajkhorshid, et al., Structural mechanism of plant aquaporin gating, Nature. 439 (2006) 688–694. http://dx.doi.org/10.1038/nature04316.

[7] C. Tournaire-Roux, M. Sutka, H. Javot, E. Gout, P. Gerbeau, D.-T. Luu, et al., Cytosolic pH regulates root water transport during anoxic stress through gating of aquaporins., Nature. 425 (2003) 393–397. doi:10.1038/nature01853.

[8] J. Bellati, K. Alleva, G. Soto, V. Vitali, C. Jozefkowicz, G. Amodeo, Intracellular pH sensing is altered by plasma membrane PIP aquaporin co-expression, Plant Mol. Biol. 74 (2010) 105–118. doi:10.1007/s11103-010-9658-8.

[9] A. Frick, M. Järvå, S. Törnroth-Horsefield, Structural basis for pH gating of plant aquaporins, FEBS Lett. 587 (2013) 989–993. doi:10.1016/j.febslet.2013.02.038.

[10] A. Yaneff, L. Sigaut, M. Marquez, K. Alleva, L.I. Pietrasanta, G. Amodeo, Heteromerization of PIP aquaporins affects their intrinsic permeability., Proc. Natl. Acad. Sci. U. S. A. 111 (2014) 231–6. http://www.ncbi.nlm.nih.gov/pubmed/24367080.

[11] I. Johansson, M. Karlsson, V.K. Shukla, M.J. Chrispeels, C. Larsson, P. Kjellbom, Water transport activity of the plasma membrane aquaporin PM28A is regulated by phosphorylation., Plant Cell. 10 (1998) 451–9. doi:10.1105/tpc.10.3.451.

[12] H.Y. Jang, J. Rhee, J.E. Carlson, S.J. Ahn, The Camelina aquaporin CsPIP2;1 is regulated by phosphorylation at Ser273, but not at Ser277, of the C-terminus and is involved in salt- and drought-stress responses, J. Plant Physiol. 171 (2014) 1401–1412. doi:10.1016/j.jplph.2014.06.009.

[13] A. Grondin, O. Rodrigues, L. Verdoucq, S. Merlot, N. Leonhardt, C. Maurel, Aquaporins contribute to ABA-triggered stomatal closure through OST1-mediated phosphorylation, Plant Cell. 27 (2015) 1945–1954. doi:10.1105/tpc.15.00421.

[14] K. Alleva, C.M. Niemietz, M. Sutka, C. Maurel, M. Parisi, S.D. Tyerman, et al., Plasma membrane of Beta vulgaris storage root shows high water channel activity regulated by cytoplasmic pH and a dual range of calcium concentrations, J. Exp. Bot. 57 (2006) 609–621. doi:10.1093/jxb/erj046.

[15] L. Verdoucq, A. Grondin, C. Maurel, Structure-function analysis of plant aquaporin AtPIP2;1 gating by divalent cations and protons., Biochem. J. 415 (2008) 409–416. doi:10.1042/BJ20080275.

[16] P. Gerbeau, G. Amodeo, T. Henzler, V. Santoni, P. Ripoche, C. Maurel, The water permeability of Arabidopsis plasma membrane is regulated by divalent cations and pH, Plant J. 30 (2002) 71–81. doi:10.1046/j.1365-313X.2002.01268.x.

[17] C. Ehlert, C. Maurel, F. Tardieu, T. Simonneau, Aquaporin-mediated reduction in Maize root hydraulic conductivity impacts cell turgor and leaf elongation even without changing transpiration, Plant Physiol. 150 (2009) 1093–1104. doi:10.1104/pp.108.131458.

[18] M. Fischer, R. Kaldenhoff, On the pH regulation of plant aquaporins, J. Biol. Chem. 283 (2008) 33889–33892. doi:10.1074/jbc.M803865200.

[19] M.C. Shelden, S.M. Howitt, B.N. Kaiser, S.D. Tyerman, Identification and functional characterisation of aquaporins in the grapevine, Vitis vinifera, Funct. Plant Biol. 36 (2009) 1065–1078. doi:10.1071/FP09117.

[20] J. Sjöhamn, K. Hedfalk, Unraveling aquaporin interaction partners, Biochim. Biophys. Acta - Gen. Subj. 1840 (2014) 1614–1623. doi:10.1016/j.bbagen.2013.11.012.

[21] L. Verdoucq, O. Rodrigues, A. Martinière, D.T. Luu, C. Maurel, Plant aquaporins on the move: reversible phosphorylation, lateral motion and cycling, Curr. Opin. Plant Biol. 22 (2014) 101–107. doi:10.1016/j.pbi.2014.09.011.

[22] A.K. Azad, M. Katsuhara, Y. Sawa, T. Ishikawa, H. Shibata, Characterization of four plasma membrane aquaporins in tulip petals: A putative homolog is regulated by phosphorylation, Plant Cell Physiol. 49 (2008) 1196–1208. doi:10.1093/pcp/pcn095.

[23] V. Van Wilder, U. Miecielica, H. Degand, R. Derua, E. Waelkens, F. Chaumont, Maize plasma membrane aquaporins belonging to the PIP1 and PIP2 subgroups are in vivo phosphorylated, Plant Cell Physiol. 49 (2008) 1364–1377. doi:10.1093/pcp/pcn112.

[24] J.C. Amezcua-Romero, O. Pantoja, R. Vera-Estrella, Ser123 is essential for the water channel activity of McPIP2;1 from Mesembryanthemum crystallinum, J. Biol. Chem. 285 (2010) 16739–16747. doi:10.1074/jbc.M109.053850.

[25] G.P. Bienert, R.B. Heinen, M.C. Berny, F. Chaumont, Maize plasma membrane aquaporin ZmPIP2;5, but not ZmPIP1;2, facilitates transmembrane diffusion of hydrogen peroxide, Biochim. Biophys. Acta - Biomembr. 1838 (2014) 216–222. doi:10.1016/j.bbamem.2013.08.011.

[26] C. Jozefkowicz, L. Sigaut, F. Scochera, G. Soto, N. Ayub, L.I. Pietrasanta, et al., PIP water transport and its pH dependence are regulated by tetramer stoichiometry, Biophys. J. 110 (2016) 1312–1321. doi:10.1016/j.bpj.2016.01.026.

[27] H.H. Felle, pH: Signal and Messenger in Plant Cells, Plant Biol. 3 (2001) 577–591. doi:10.1055/s-2001-19372.

[28] S. Prak, S. Hem, J. Boudet, G. Viennois, N. Sommerer, M. Rossignol, et al., Multiple phosphorylations in the C-terminal tail of plant plasma membrane aquaporins: role in subcellular trafficking of AtPIP2;1 in response to salt stress., Mol. Cell. Proteomics. 7 (2008) 1019–1030. doi:10.1074/mcp.M700566-MCP200.

[29] S.A. Whiteman, T.S. Nühse, D. a. Ashford, D. Sanders, F.J.M. Maathuis, A proteomic and phosphoproteomic analysis of Oryza sativa plasma membrane and vacuolar membrane, Plant J. 56 (2008) 146–156. doi:10.1111/j.1365-313X.2008.03578.x.

[30] K.G. Kline, G. a Barrett-Wilt, M.R. Sussman, In planta changes in protein phosphorylation induced by the plant hormone abscisic acid., Proc. Natl. Acad. Sci. U. S. A. 107 (2010) 15986–15991. doi:10.1073/pnas.1007879107.

[31] X.N. Wu, C. Sanchez Rodriguez, H. Pertl-Obermeyer, G. Obermeyer, W.X. Schulze, Sucrose-induced receptor kinase SIRK1 regulates a plasma membrane aquaporin in Arabidopsis., Mol. Cell. Proteomics. 12 (2013) 2856–73. doi:10.1074/mcp.M113.029579.

[32] M. di Pietro, J. Vialaret, G.-W. Li, S. Hem, K. Prado, M. Rossignol, et al., Coordinated post-translational responses of aquaporins to abiotic and nutritional stimuli in Arabidopsis roots., Mol. Cell. Proteomics. 12 (2013) 3886–97. doi:10.1074/mcp.M113.028241.

[33] J. Casado-Vela, B. Muries, M. Carvajal, I. Iloro, F. Elortza, M.C. Mart??nez-Ballesta, Analysis of root plasma membrane aquaporins from brassica oleracea: Post-translational modifications, de novo sequencing and detection of isoforms by high resolution mass spectrometry, J. Proteome Res. 9 (2010) 3479–3494. doi:10.1021/pr901150g.

[34] P. Mut, C. Bustamante, G. Martínez, K. Alleva, M. Sutka, M. Civello, et al., A fruit-specific plasma membrane aquaporin subtype PIP1;1 is regulated during strawberry (Fragaria x ananassa) fruit ripening, Physiol. Plant. 132 (2008) 538–551. doi:10.1111/j.1399-3054.2007.01046.x.

[35] K. Alleva, M. Marquez, N. Villarreal, P. Mut, C. Bustamante, J. Bellati, et al., Cloning, functional characterization, and co-expression studies of a novel aquaporin (FaPIP2;1) of strawberry fruit, J. Exp. Bot. 61 (2010) 3935–3945. doi:10.1093/jxb/erq210.

[36] R.B. Zhang, A.S. Verkman, Water and urea permeability properties of Xenopus oocytes: expression of mRNA from toad urinary bladder., Am. J. Physiol. 260 (1991) C26–C34.

[37] G.M. Preston, T.P. Carroll, W.B. Guggino, P. Agre, Appearance of water channels in Xenopus oocytes expressing red cell CHIP28 protein., Science. 256 (1992) 385–387. doi:DOI:10.1126/science.256.5055.385.

[38] C. Jozefkowicz, P. Rosi, L. Sigaut, G. Soto, L.I. Pietrasanta, G. Amodeo, et al., Loop A

Is critical for the functional interaction of two Beta vulgaris PIP aquaporins, PLoS One. 8(3):e5799 (2013). doi:10.1371/journal.pone.0057993.

[39] Y. Temmei, S. Uchida, D. Hoshino, N. Kanzawa, M. Kuwahara, S. Sasaki, et al., Water channel activities of Mimosa pudica plasma membrane intrinsic proteins are regulated by direct interaction and phosphorylation, FEBS Lett. 579 (2005) 4417–4422. doi:10.1016/j.febslet.2005.06.082.

[40] I. Johansson, M. Karlsson, V.K. Shukla, M.J. Chrispeels, C. Larsson, P. Kjellbom, Water transport activity of the plasma membrane aquaporin PM28A is regulated by phosphorylation., Plant Cell. 10 (1998) 451–459. doi:10.1105/tpc.10.3.451.

[41] E.J. Kamsteeg, I. Heijnen, C.H. Van Os, P.M.T. Deen, The subcellular localization of an aquaporin-2 tetramer depends on the stoichiometry of phosphorylated and nonphosphorylated monomers, J. Cell Biol. 151 (2000) 919–929. doi:10.1083/jcb.151.4.919.

[42] J. Cui, BK-type calcium-activated potassium channels: coupling of metal ions and voltage sensing., J. Physiol. 588 (2010) 4651–4658. doi:10.1113/jphysiol.2010.194514.

[43] K. Sakano, Metabolic regulation of pH in plant cells: Role of cytoplasmic pH in defense reaction and secondary metabolism, Int. Rev. Cytol. 206 (2001) 1–44. doi:10.1016/S0074-7696(01)06018-1.

[44] M. Katsuhara, K. Kuchitsu, K. Takeshige, M. Tazawa, Salt stress-induced cytoplasmic acidification and vacuolar alkalization in Nitellopsis obtusa cells : In Vivo P-nuclear magnetic resonance study, Plant Physiol. 90 (1989) 1102–1107. doi:10.1104/pp.90.3.1102.

[45] A. Martinière, E. Bassil, E. Jublanc, C. Alcon, M. Reguera, H. Sentenac, et al., In vivo intracellular pH measurements in tobacco and Arabidopsis reveal an unexpected pH gradient in the endomembrane system., Plant Cell. 25 (2013) 4028–43. doi:10.1105/tpc.113.116897.

[46] A. Martinière, G. Desbrosses, H. Sentenac, N. Paris, Development and properties of genetically encoded pH sensors in plants., Front. Plant Sci. 4 (2013) 523. doi:10.3389/fpls.2013.00523.

[47] T. Niittylä, A.T. Fuglsang, M.G. Palmgren, W.B. Frommer, W.X. Schulze, Temporal analysis of sucrose-induced phosphorylation changes in plasma membrane proteins of Arabidopsis., Mol. Cell. Proteomics. 6 (2007) 1711–1726. doi:10.1074/mcp.M700164-MCP200.

[48] D. Qing, Z. Yang, M. Li, W.S. Wong, G. Guo, S. Liu, et al., Quantitative and functional phosphoproteomic analysis reveals that ethylene regulates water transport via the C-Terminal phosphorylation of aquaporin PIP2;1 in Arabidopsis, Mol. Plant. 9 (2016) 158–174. doi:10.1016/j.molp.2015.10.001.

[49] K. Prado, Y. Boursiac, C. Tournaire-Roux, J.-M. Monneuse, O. Postaire, O. Da Ines, et al., Regulation of Arabidopsis leaf hydraulics involves light-dependent phosphorylation of aquaporins in veins., Plant Cell. 25 (2013) 1029–39. doi:10.1105/tpc.112.108456.

[50] T.S. Nühse, A. Stensballe, O.N. Jensen, S.C. Peck, Phosphoproteomics of the Arabidopsis plasma membrane and a new phosphorylation site database., Plant Cell. 16 (2004) 2394–2405. doi:10.1105/tpc.104.023150.

[51] S.A. Whiteman, L. Serazetdinova, A.M.E. Jones, D. Sanders, J. Rathjen, S.C. Peck, et al., Identification of novel proteins and phosphorylation sites in a tonoplast enriched membrane fraction of Arabidopsis thaliana, Proteomics. 8 (2008) 3536–3547. doi:10.1002/pmic.200701104.

[52] J.L. Hsu, L.Y. Wang, S.Y. Wang, C.H. Lin, K.C. Ho, F.K. Shi, et al., Functional phosphoproteomic profiling of phosphorylation sites in membrane fractions of salt-stressed Arabidopsis thaliana, Proteome Sci. 7 (2009) 42. doi:10.1186/1477-5956-7-42.

[53] R. Aroca, G. Amodeo, S. Fernández-Illescas, E.M. Herman, F. Chaumont, M.J. Chrispeels, The role of aquaporins and membrane damage in chilling and hydrogen peroxide induced changes in the hydraulic conductance of maize roots., Plant Physiol. 137 (2005) 341–53. doi:10.1104/pp.104.051045.

[54] S. Sjövall-Larsen, E. Alexandersson, I. Johansson, M. Karlsson, U. Johanson, P. Kjellbom, Purification and characterization of two protein kinases acting on the aquaporin SoPIP2;1, Biochim. Biophys. Acta - Biomembr. 1758 (2006) 1157–1164. doi:10.1016/j.bbamem.2006.06.002.

Figure Legends

Fig. 1. P_f inhibitory response of FaPIP2;1 triggered by the combination of cytosolic acidification and K252a. **(A)** Oocytes were injected with 2 ng of FaPIP2;1 cRNA and submitted to a 30 minute incubation in different solutions. P_f values of columns 2, 3, 4, 5 are not significantly different. Incubation with a sodium acetate solution at pH=6.3 triggered a cytosolic acidification of the oocytes to pH_i=6.6. FaPIP2;1 P_f inhibition was not observed at this pH (Column 3) and also K252a did not produce a significant decrease on P_f (Column 5). DMSO 0.1% was used as vehicle and did not affect P_f since no significant differences were observed between the P_f of oocytes incubated with the sodium acetate solution at pH=7.4 (Column 2) and the same solution with DMSO 0.1% (Column 4). The combination of pH=6.3 sodium acetate and K252a 1 µM diminish the P_f near 50% proving a synergic action of both treatments (a-b, $p<0.05$, n= 8-12). Data are expressed as mean values (mean P_f ± SEM,). (**B**) P_f vs. $[H^+]$ inhibitory response profile for oocytes injected with 2 µg of FaPIP2;1 cRNA subjected or not to 30 minutes incubation with K252a 1 µM. The data points are representative values obtained from the same batch of oocytes (mean P_f ± SEM). Data were fitted to an allosteric sigmoidal dose–response curve described by Equation 1. (**C**) The EC_{50} values are reported as the average (EC_{50} ± SEM) for each treatment. Means are significantly different ($p<0.005$, n=3-5) (**D**) K_I values are reported as the average (K_I ± SEM) for each treatment. Means are significantly different ($p<0.005$, n=3-5).

Fig. 2. Trafficking to Xenopus oocyte plasma membrane is less effective for FaPIP2;1S121A than for FaPIP2;1 wt. **(A)** P_f values of oocytes injected with three different masses of FaPIP2;1S121A cRNA. Non-injected oocytes (NI) and oocytes injected with FaPIP2;1 cRNA were used as negative and positive controls respectively. Values are expressed as mean P_f ± SEM. P_f mean value of oocytes injected with 10 ng of cRNA is significantly different to the P_f mean value of non-injected oocytes (*, $p<0.05$, n= 11-13.). **(B)** and **(C)** Subcellular localization of FaPIP2;1S121A-EYFP injected with 2.50 ng and 10.00 ng of cRNA respectively. Confocal images (x-z) of *Xenopus laevis* oocytes expressing FaPIP2;1S121A-EYFP, previously injected with a cytosolic marker, TMR-dextran (red). The oocyte surface is shown near the right of each image frame, and the interior of the oocyte is to the left. Insets show an enlargement of the indicated square section. As a reference for subcellular localization,

average difference profiles for oocytes expressing FaPIP1;1-YFP (reference for interior localization) or FaPIP2;1-EYFP (reference for PM localization) are presented in **(D)**. **(E)** and **(F)** Top panel, normalized intensity profiles for the indicated EYFP-aquaporin (black line) and TMR-dextran (red line) from images presented in (**B**) and (**C**); bottom panel, difference profile calculated as the difference between the normalized EYFP-aquaporin and TMR-dextran profiles. Out/in indicate outside or inside the oocyte. When oocytes were injected with low amounts of FaPIP2;1S121A-EYFP cRNA, the fluorescence is mainly visualized in intracellular structures (**B**) and the difference average profile is in agreement with interior localization (**E**). If the amount of cRNA injected is increased, the fluorescence is more probable to be visualized both in PM and in intracellular structures (**C**) and difference profile is consistent with PM localization (**F**). See also Suppl. Fig. 2.

Fig. 3. FaPIP2;1S121A-EYFP is located in the PM when it is co-expressed with FaPIP2;1. (**A**) P_f of oocytes injected with 1.25 ng and 2.50 ng of cRNA of FaPIP2;1 were measured and compared to the P_f values obtained for the co-injection of 1.25 ng of cRNA of FaPIP2;1 with 1.25 ng of cRNA of FaPIP2;1S121A. P_f values are expressed as mean P_f ± SEM, P_f mean value of oocytes injected with 1.25 ng of FaPIP2;1 cRNA is significantly different to the P_f mean value of oocytes injected with 1.25 ng of FaPIP2;1 cRNA plus 1.25 ng of FaPIP2;1S121A cRNA (**, $p<0.005$, n=10-15). (**B**) Subcellular localization of FaPIP2;1S121A-EYFP co-expressed with FaPIP2;1. Confocal image (x-z) of *Xenopus laevis* oocytes expressing FaPIP2;1S121A-EYFP (green) with FaPIP2;1, previously injected with TMR- dextran (red). See also Suppl. Fig. 2.

Fig. 4. FaPIP2;1S121A presents functional interaction with FaPIP1;1 and both achieve the plasma membrane due to their interaction. (AB) Confocal images (x-z) of *Xenopus laevis* oocytes expressing (**A**) FaPIP2;1S121A-EYFP (green) with FaPIP1;1 or (**B**) FaPIP1;1-EYFP (green) with FaPIP2;1S121A, previously injected -in both cases- with TMR-dextran (red). (**A**) FaPIP2;1S121A-EYFP is located in the plasma membrane of the oocyte when it is co-expressed with FaPIP1;1. (**B**) FaPIP1;1-EYFP is located in the plasma membrane of the oocyte when it is co-expressed with FaPIP2;1S121A. (**C**) P_f values of oocytes co-expressing FaPIP1;1 with the corresponding loop B Serine mutant. P_f mean value of oocytes injected with FaPIP2;1S121A cRNA is significantly different than the P_f mean value of oocytes co-injected with FaPIP1;1 and FaPIP2;1S121A cRNAs ($p<0.005$, n=8-12). P_f mean value of oocytes co-injected with FaPIP1;1 and FaPIP2;1 cRNAs is significantly different than the P_f mean value of

oocytes co-injected with FaPIP1;1 and FaPIP2;1S121A cRNAs ($p<0.005$, n=8-12).The amount of cRNA is represented in parentheses (arbitrary unit of measure, where 1 is equivalent to 1.25 ng of cRNA). P_f values are expressed as mean P_f ± SEM. See also Suppl. Fig. 2.

Fig. 5. FaPIP2;1S121A gating is more sensitive to an increase of cytosolic proton concentration than FaPIP2;1. (**A**) P_f vs. $[H^+]$ inhibitory response profile for oocytes injected with FaPIP2;1 or FaPIP2;1S121A cRNA. The amount of cRNA is represented in parentheses (arbitrary unit of measure, where 1 is equivalent to 1.25 ng of cRNA). The data points are representative values obtained from the same batch of oocytes (mean P_f ± SEM). Data were fit to an allosteric sigmoidal dose–response curve described by Equation 1. (**B**) The EC_{50} values are reported as the average of different independent experiments (EC_{50} ± SEM, n = 3–5) for each treatment. FaPIP2;1 EC_{50} value is not significantly different from the value obtained in previous work [10]. (**C**) K_I values are reported as the average of different independent experiments (K_I ± SEM, n = 3–5). Both K_I and EC_{50} are significantly different between treatments ($p<0.005$, n=3-5)

Fig. 6. Interaction between FaPIP1;1 and FaPIP2;1S121A cooperatively increase proton sensitivity shifting the EC_{50} to a higher pH. (**A**) P_f vs. $[H^+]$ inhibitory response profile for oocytes co-injected with FaPIP1;1 with FaPIP2;1 or FaPIP2;1S121A cRNA. The amount of cRNA is represented in parentheses (arbitrary unit of measure, where 1 is equivalent to 1.25 ng of cRNA). The data points are representative values obtained from the same batch of oocytes (mean P_f ± SEM). Data were fit to an allosteric sigmoidal dose–response curve described by Equation 1. (**B**) The EC_{50} values reported as the average of different independent experiments for each treatment (EC_{50} ± SEM). Means are significantly different (n=4, $p<0.005$). (**C**) K_I values are reported as the average of different independent experiments for each treatment (K_I ± SEM). Means are significantly different (n=4, $p<0.005$).

Fig. 7. FaPIP1;1S131A has the same $[H^+]$ gating sensitivity than FaPIP1;1. (**A**) P_f values of oocytes co-expressing FaPIP2;1 with the corresponding FaPIP1;1 loop B Serine mutant. P_f mean value of oocytes injected with FaPIP1;1S131A cRNA is significantly different than the P_f mean value of oocytes co-injected with FaPIP1;1S131A and FaPIP2;1 cRNAs ($p<0.005$, n=9-10). P_f mean value of oocytes co-injected with FaPIP1;1 and FaPIP2;1 cRNAs is significantly different than the P_f mean value of oocytes co-injected with FaPIP1;1S131A and FaPIP2;1 cRNAs ($p<0.005$, n=9-10). The amount of cRNA is represented in parentheses (arbitrary unit of measure,

where 1 is equivalent to 1.25 ng of cRNA). P_f values are expressed as mean P_f ± SEM, n= 8-12. (**B**) P_f vs. [H^+] inhibitory response profile for oocytes co-injected with FaPIP2;1 and FaPIP1;1S131A or FaPIP1;1 cRNA. P_f values are expressed as mean P_f ± SEM, n = 8-12. The amount of cRNA is represented in parentheses (arbitrary unit of measure, where 1 is equivalent to 1.25 ng of cRNA). The data points are representative values obtained from the same batch of oocytes (mean P_f ± SEM). Data were fit to an allosteric sigmoidal dose–response curve described by Equation 1. (**C**) EC_{50} values reported as the average of three to five independent experiments for each treatment. (EC_{50} ± SEM). (**D**) K_I values are reported as the average of different independent experiments for each treatment (K_I ± SEM). Both K_I and EC_{50} are not significantly different between treatments (n=3-5).

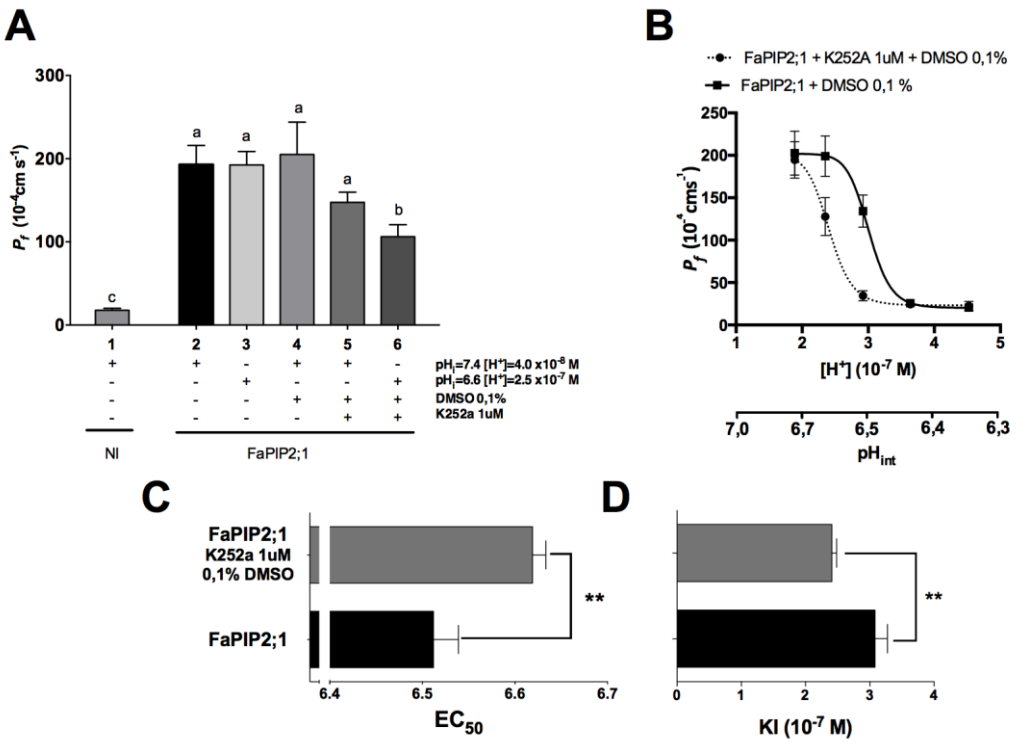

Figure 1

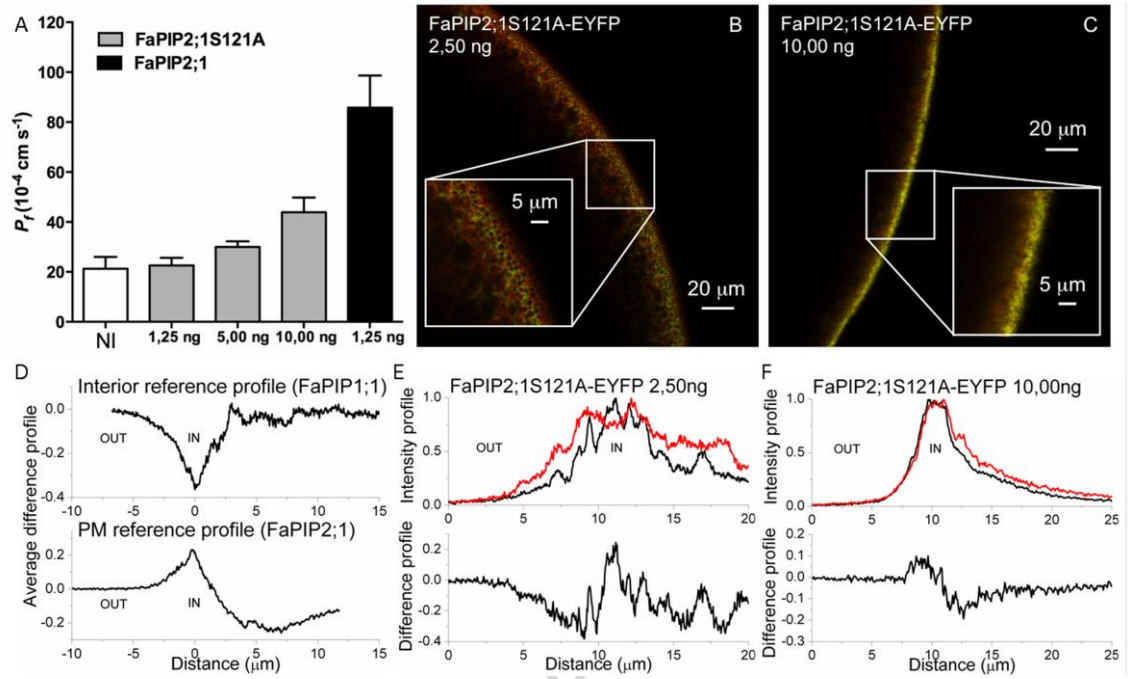

Figure 2

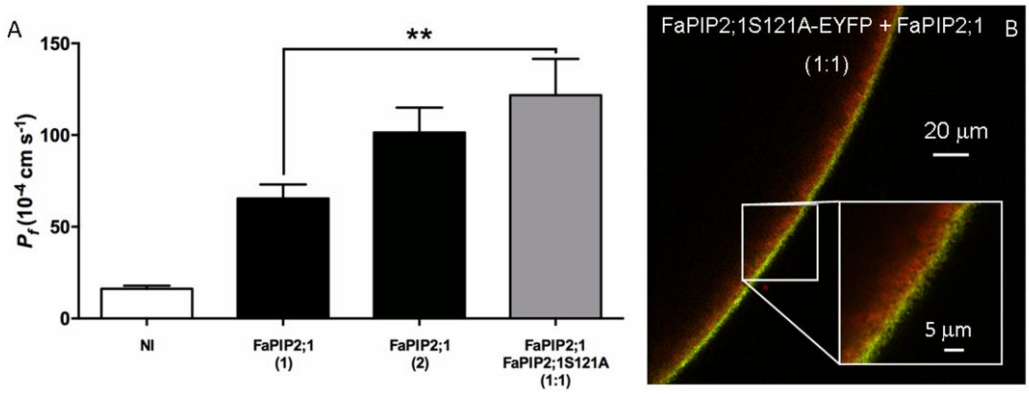

Figure 3

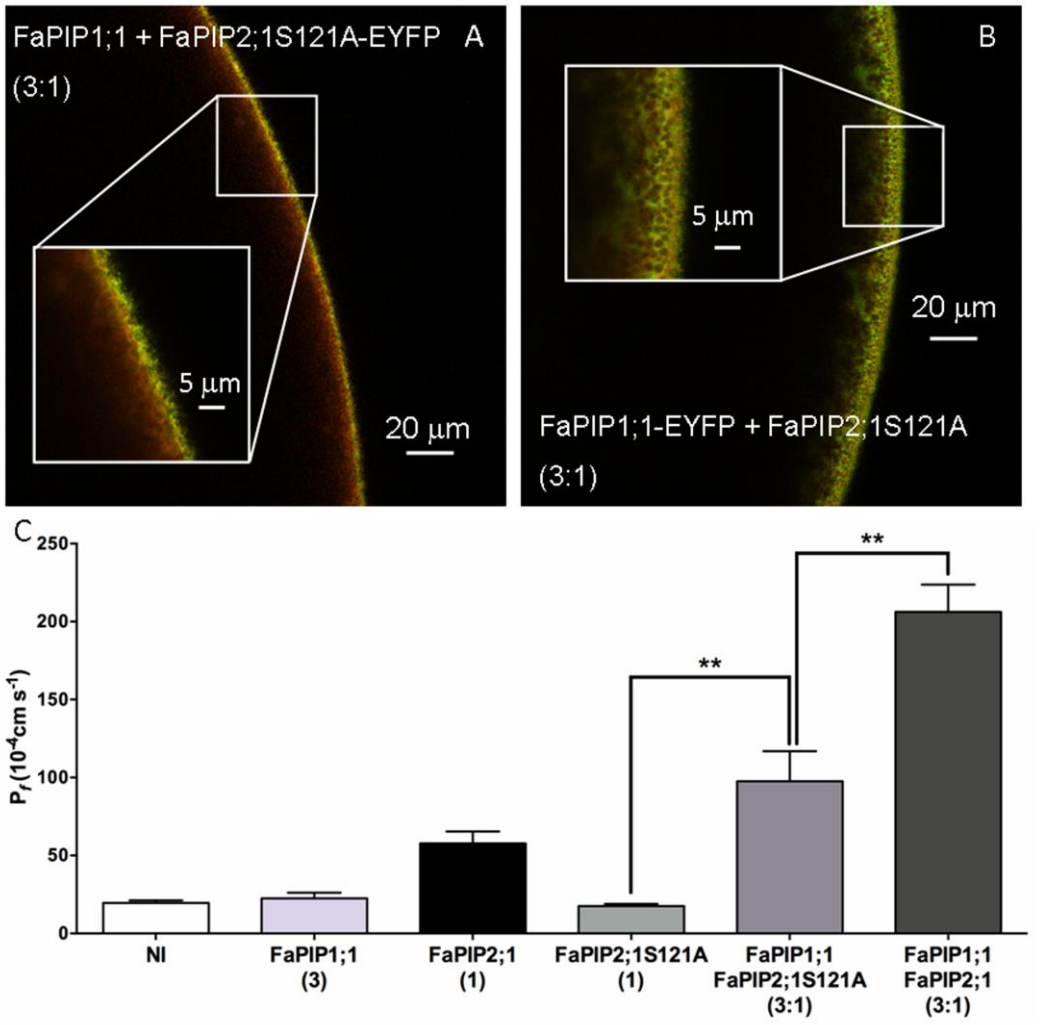
FaPIP1;1 + FaPIP2;1S121A-EYFP
(3:1)
A
5 µm
20 µm
B
5 µm
20 µm
FaPIP1;1-EYFP + FaPIP2;1S121A
(3:1)
C
P_f (10^{-4}cm s^{-1})
250
200
150
100
50
0
**
**
NI
FaPIP1;1 (3)
FaPIP2;1 (1)
FaPIP2;1S121A (1)
FaPIP1;1 FaPIP2;1S121A (3:1)
FaPIP1;1 FaPIP2;1 (3:1)

Figure 4

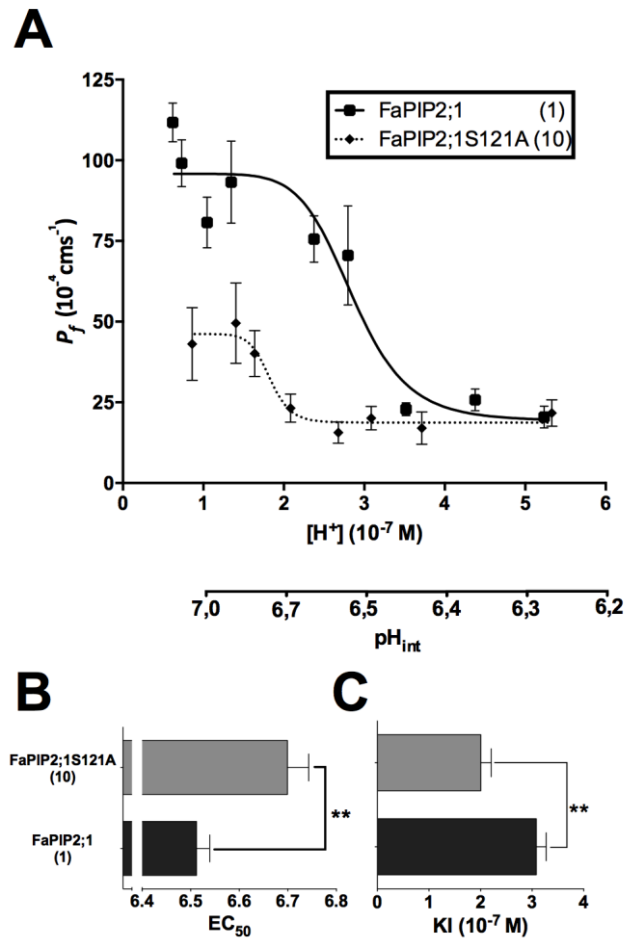

Figure 5

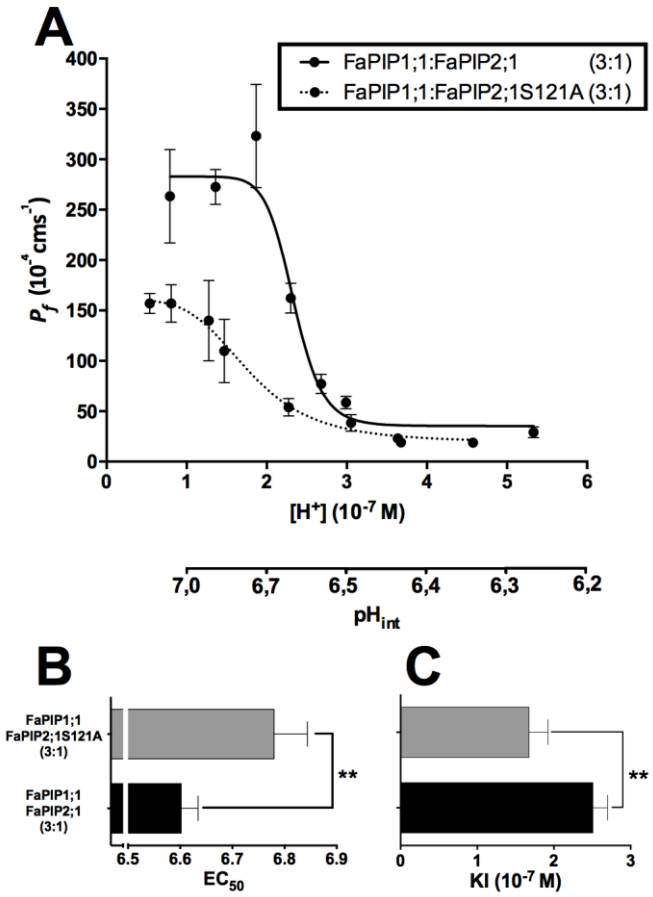

Figure 6

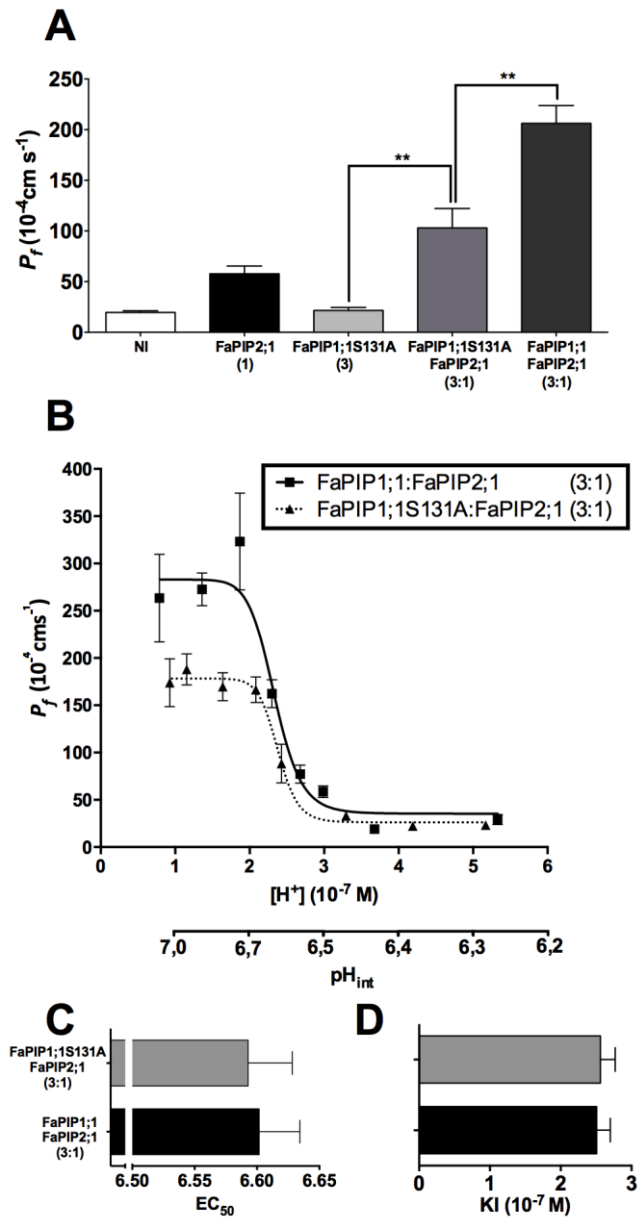

Figure 7

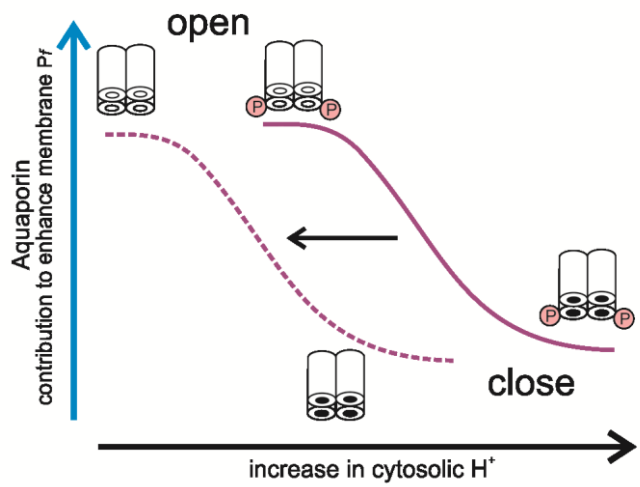

Graphical abstract